

## Triaxial bands in $^{133}\text{Ce}$

K. Hauschild,\* R. Wadsworth, R. M. Clark,† and I. M. Hibbert  
*Department of Physics, University of York, Heslington, York, YO1 5DD, United Kingdom*

P. Fallon and A. O. Macchiavelli  
*Nuclear Science Division, Lawrence Berkeley National Laboratory, Berkeley, California 94720*

D. B. Fossan, H. Schnare,‡ and I. Thorslund  
*Department of Physics, State University of New York, Stony Brook, New York 11794*

P. J. Nolan, A. T. Semple, and L. Walker  
*Oliver Lodge Laboratory, University of Liverpool, Liverpool, L69 3BX, United Kingdom*

(Received 25 January 1996)

An experiment performed on the early implementation of the GAMMASPHERE array to populate the high-spin states in  $^{133}\text{Ce}$  has revealed the presence of several rotational structures with energy spacings of  $\Delta E_\gamma \sim 100$  keV. Some of these bands exhibit a backbend at  $\hbar\omega \sim 0.6$  MeV and are observed to high rotational frequencies— $\hbar\omega \sim 0.85$  MeV. These characteristics are very different from those observed for any other rotational bands in this mass region. The properties of these new structures will be discussed within the framework of cranked Strutinsky-Woods-Saxon calculations. Currently, these bands are thought to be based on triaxial nuclear shapes. [S0556-2813(96)05708-1]

PACS number(s): 27.60.+j, 23.20.Lv, 21.10.Re, 21.60.Ev

### I. INTRODUCTION

It is now well established in the mass  $A \sim 130$  region that rotational structures with large differences in  $\beta_2$  and  $\gamma$  deformation parameters coexist within the same nucleus. The transitional  $A \sim 130$  nuclei, lying above the  $Z=50$ , and below the  $N=82$  shell closures are predicted to have  $\gamma$ -soft cores [1–4]. Consequently, the nuclear shape can be stabilized at different specific  $\gamma$  values by the occupation of different high- $j$  quasiparticle orbitals [5]. The shape driving effects of these quasiparticles are highly dependent upon the position of the Fermi surface within the shell. When the surface is at the bottom of the shell, prolate shapes,  $\gamma \sim 0^\circ$  (Lund convention [6]), will be favored, while oblate shapes,  $\gamma \sim -60^\circ$ , are preferred when the Fermi surface lies at the top of the shell. Thus, for cerium isotopes with neutron number  $N > 74$ , the occupation of low- $\Omega$   $h_{11/2}$  quasiproton orbitals have the opposite gamma-driving effect on the nuclear core to the high- $\Omega$   $h_{11/2}$  quasineutron orbitals. In the  $N=75$  and  $N=77$  cerium isotopes, which possess significant triaxiality ( $\gamma \sim -30^\circ$ ) in their low spin yrast states [7,8], the rotational alignment of both  $\pi(h_{11/2})^2$  and  $\nu(h_{11/2})^2$  quasiparticles are predicted to occur at similar rotational frequencies. The rotational alignment of these pairs of high- $j$  intruder orbitals is expected to strongly influence the nuclear shape. In addition, at high excitation energies and spins the

existence of superdeformed structures corresponding to collective rotations of a strongly deformed prolate shape ( $\beta_2 \sim 0.4$ ) have been known for several years in nuclei around mass 130, e.g. [9,10]. Three such bands have been recently identified in  $^{133}\text{Ce}_{75}$  [11]. This offers an excellent opportunity to study the phenomena of shape coexistence in these nuclei.

In this paper we present new results for the  $^{133}\text{Ce}$  isotope obtained with the early implementation of the GAMMASPHERE spectrometer array situated at the Lawrence Berkeley National Laboratory. Six new rotational structures with energy spacings of  $\Delta E_\gamma \sim 100$  keV have been observed, some of which exhibit a backbend at  $\hbar\omega \sim 0.6$  MeV and extend to high rotational frequency ( $\hbar\omega \approx 0.85$  MeV). These new  $\Delta E_\gamma \sim 100$  keV bands possess similar dynamic moments of inertia to a known rotational band in  $^{133}\text{Ce}$  [7] which has a measured transitional quadrupole moment  $Q_t \approx 2.3$  e b [12]. This value is markedly different from those measured for the prolate superdeformed bands in this nucleus,  $Q_t = 7.5 \pm 0.8$  ( $\beta_2 = 0.41 \pm 0.4$ ) [13]. The properties of these  $\Delta E_\gamma \sim 100$  keV bands will be discussed within the framework of cranked Strutinsky-Woods-Saxon calculations.

### II. EXPERIMENTAL DETAILS

High-spin states in  $^{133}\text{Ce}$  were populated via the  $^{116}\text{Cd}$  ( $^{22}\text{Ne}, 5n$ ) fusion-evaporation reaction at a beam energy of 120 MeV. The beam, provided by the 88-in. Cyclotron at the Lawrence Berkeley National Laboratory, was incident upon two  $500 \mu\text{g cm}^{-2}$  self-supporting  $^{116}\text{Cd}$  targets. Coincident gamma rays emitted during the decay of these high-spin states were detected with the early implementation phase of the GAMMASPHERE array which, for this experiment, consisted of 31 large-volume (75–80 % efficient) HpGe Comp-

\*Present address: Lawrence Livermore National Laboratory, Livermore, CA 94550.

†Present address: Lawrence Berkeley National Laboratory, Berkeley, CA 94720.

‡Present address: Research Centre Rossendorf, PF 510119, D-01314 Dresden, Germany.

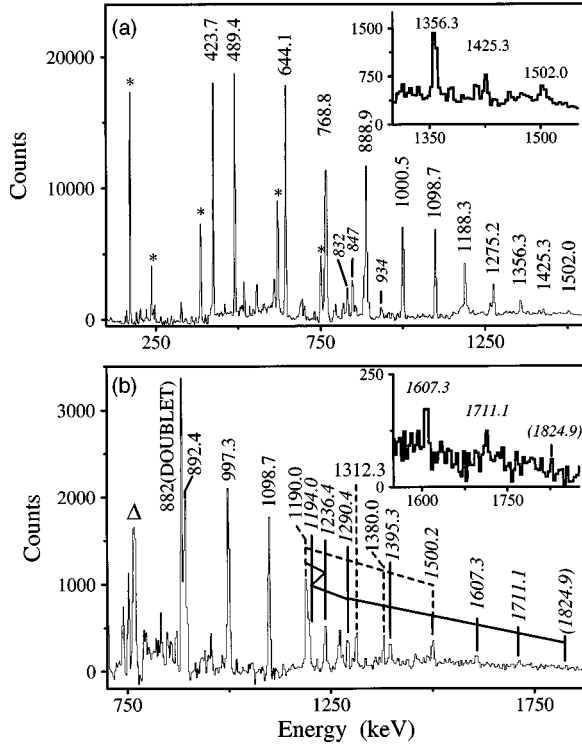


FIG. 1. Spectra obtained as a result of all possible combinations of double gates on the members of (a) triaxial band 1 and (b) triaxial bands 2 and 3 within a Radware cube. In (a) the low-lying transitions of  $^{133}\text{Ce}$  are marked by an asterisk, while those transitions observed in coincidence with band 1 and the  $\nu h_{11/2}$  band are labeled in italics. In (b) triaxial band 3 is labeled in italics and the 768.1 keV transition in triaxial band one is indicated by a  $\Delta$ . All transitions are labeled in keV.

ton escape-suppressed detectors [14]. Approximately  $1.5 \times 10^9$  events were recorded with a suppressed Ge-fold  $\geq 3$ . These data were unpacked into doubles and sorted into a standard  $E_{\gamma 1} - E_{\gamma 2}$  matrix. Using the triples data, the  $^{133}\text{Ce}$  reaction channel was enhanced by demanding that one of these  $\gamma$  rays was an uncontaminated low-lying transition in  $^{133}\text{Ce}$ . The remaining two coincident  $\gamma$  rays were then incremented into an  $E_{\gamma 1} - E_{\gamma 2}$  matrix. The unpacked triples data were also sorted into an  $E_{\gamma 1} - E_{\gamma 2} - E_{\gamma 3}$  RADWARE cube [15].

### III. RESULTS

Using a variable-spaced lattice search analysis [16] performed on the present  $^{133}\text{Ce}$  gated matrix, six new weakly populated rotational sequences with energy spacings of  $\Delta E_{\gamma} \sim 100$  keV have been extracted, in addition to the three superdeformed bands reported in [11]. These bands have been assigned to  $^{133}\text{Ce}$  from observed coincidence relationships with known low-lying transitions [7]. Examples of  $\gamma$ -ray spectra for these new structures are presented in Figs. 1 and 2, which are the result of all possible combinations of double gates on the members of each band from a RADWARE cube. The cascade shown in Fig. 1(a) has been reported previously in Refs. [7] and [17]. The remaining rotational bands, triaxial bands 2–7, are new. The main feature common to these bands is the relatively large transition en-

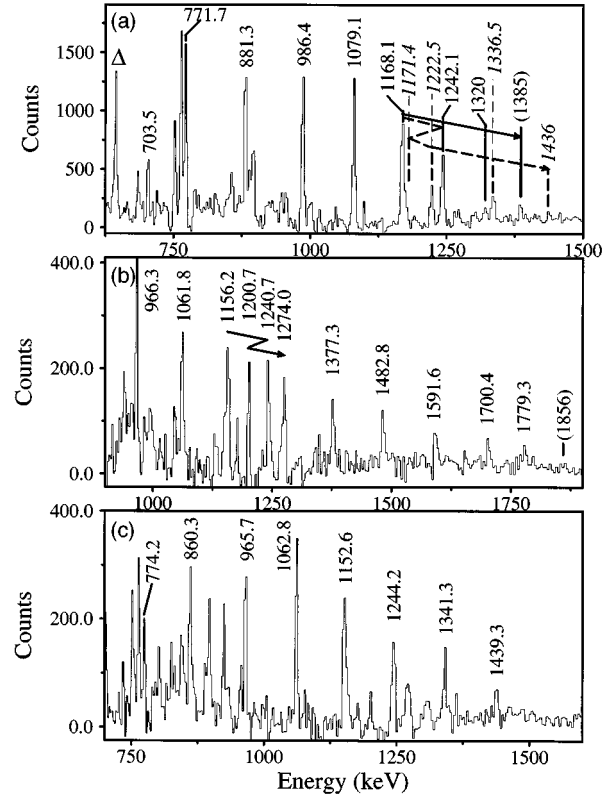


FIG. 2. Spectra obtained from a Radware cube as a result of all possible combinations of double gates on the members of (a) triaxial bands 4 and 5, (b) band 6, and (c) band 7. In (a) the transitions of band 5 are marked in italics and the 644.1 keV transition in triaxial band one is indicated by a  $\Delta$ . All transitions are labeled in keV.

ergy spacing,  $\Delta E_{\gamma} \sim 100$  keV. Furthermore, some of the bands exhibit a backbend at  $\hbar\omega \sim 0.6$  MeV and are observed to high rotational frequency,  $\hbar\omega \sim 0.85$  MeV. These characteristics are very different from those of the superdeformed bands reported in this mass region and consequently the  $\Delta E_{\gamma} \sim 100$  keV bands are expected to have a somewhat different structure.

The intensities of the  $\Delta E_{\gamma} \sim 100$  keV bands relative to the total population of  $^{133}\text{Ce}$  have been estimated using single gates from double coincidences to be  $\sim 10\%$  for band 1,  $\sim 2\%$  and  $\sim 1.5\%$  for bands 2 and 4, respectively, and  $\sim 0.5\%$  for bands 3, 5, 6, and 7. With the exception of band 1, these bands are populated with intensities very similar to those of the superdeformed bands observed in this nucleus. An intriguing feature is that even with the high selectivity available from the high-fold data of the GAMMASPHERE array it has not proved possible to either, confirm the existence of the decay paths linking band 1 and the low-lying states indicated in Ref. [7] or, to determine any other definite decay path from this band. This is surprising given the intensity of this band ( $\sim 10\%$ ) and leads us to believe that the bandhead of this sequence may be an isomeric state. However, transitions with energies 832, 847, 934, and 1177 keV have been observed in coincidence with band 1 and the low-lying yrast  $\nu h_{11/2}$  band (labeled B1 in Fig. 3), and it may be possible to link these into the level scheme at a later date. It has also not been possible to observe transitions linking the

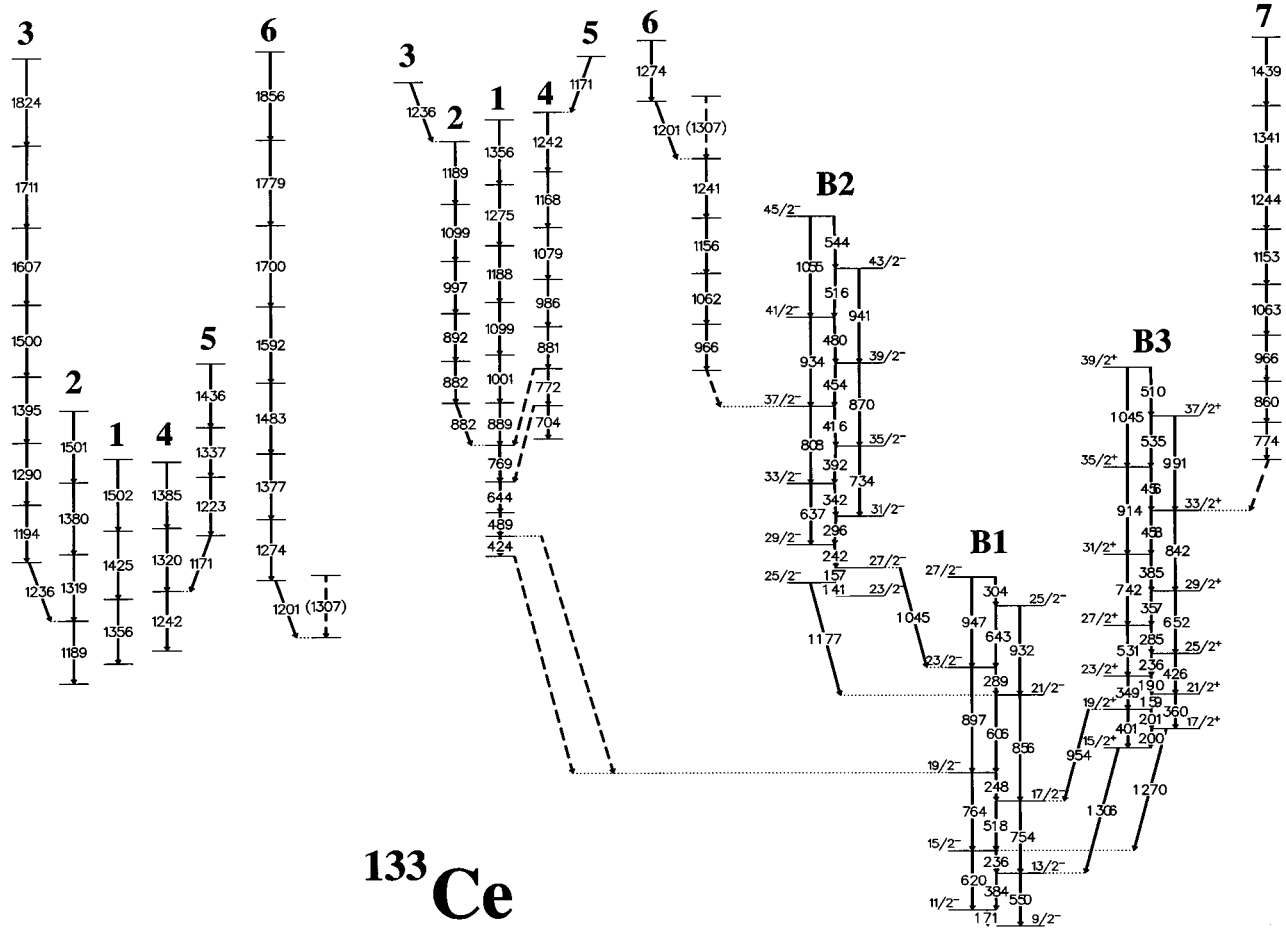


FIG. 3. Predominant decay paths between the newly discovered  $\Delta E_\gamma \sim 100$  keV bands and the previously known low-lying states in  $^{133}\text{Ce}$ . Transition energies are given in keV. The right part shows the lower portion of the level scheme, while the left-hand side displays the extension of these bands up to the highest observed states.

other  $\Delta E_\gamma \sim 100$  keV rotational bands to the normal deformed states. Consequently, the excitation energies, spins and parities of states in the bands are not known. However, the primary decay paths of the newly discovered  $\Delta E_\gamma \sim 100$  keV bands into the previously known low-lying states are shown in Fig. 3. Assuming that the lowest observed state in band 1 is the  $I = 27/2\hbar$  bandhead (see discussion in Sec. IV A) and that the unseen linking transitions between band 6 and the band labeled B2 in Fig. 3 also contribute  $\sim 4\hbar$  to the total spin, then bands 3 and 6 are observed up to approximately spin  $99/2\hbar$  and  $93/2\hbar$ , respectively. In obtaining this estimate it was also assumed that the in-band transitions are stretched E2's. Although it has not proved possible to perform a directional correlation (DCO) analysis for these bands from the GAMMASPHERE data because of insufficient statistics detected at  $90^\circ$  relative to the beam axis, the intensity ratios  $I(136^\circ, 57^\circ)/I(57^\circ, 136^\circ)$  have been extracted for band 1 [7] indicating the  $\Delta I = 2$  nature of the in-band transitions. The other  $\Delta E_\gamma \sim 100$  keV bands have also been assumed to be  $\Delta I = 2$  bands. An excellent example of shape coexistence is therefore exhibited in  $^{133}\text{Ce}$ , with the  $\Delta E_\gamma \sim 100$  keV bands competing in intensity, excitation energy and spin with the superdeformed bands.

#### IV. DISCUSSION

The new  $\Delta E_\gamma \sim 100$  keV bands reported in this work are the first of this type to be observed in the mass 130 region. At the present time both the uniqueness of these structures to  $^{133}\text{Ce}$  and the rather large number of bands observed makes it difficult to assign configurations. If detailed searches in existing data sets were to establish the occurrence of similar bands in neighboring nuclei, then it could be possible to invoke blocking arguments to facilitate the configuration assignments. However, at present it is only possible to interpret the current findings using the results of total Routhian surface and cranked Woods-Saxon calculations for  $^{133}\text{Ce}$ . These calculations predict that at low frequencies,  $\hbar\omega < 0.23$  MeV, the yrast minimum at  $\beta_2 \sim 0.18$  and  $\gamma \sim -30^\circ$  corresponds to the valence neutron occupying the  $[514]9/2^-$  orbital; see Fig. 4(a). This configuration has been previously assigned [7] to the low-lying  $\nu h_{11/2}$  band. The negative parity band built on the  $23/2^-$  state, labeled B2 in Fig. 3, has been assigned a  $\nu h_{11/2} \otimes \pi(h_{11/2})^2$  configuration, while the positive parity band, labeled B3, built on the  $15/2^+$  level was assigned a  $\nu h_{11/2} \otimes \pi h_{11/2} \otimes \pi g_{7/2}$  structure [7]. Cranked Woods-Saxon calculations performed with pairing for  $^{133}\text{Ce}$  using the deformation parameters  $\beta_2 = 0.18$  and

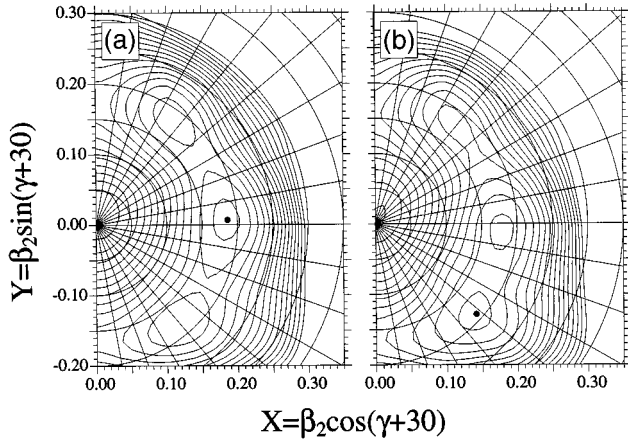


FIG. 4.  $^{133}\text{Ce}$  total Routhian surface calculations with the odd neutron occupying the lowest  $(\pi, \alpha) = (-, -\frac{1}{2})$  orbital. (a)  $\omega = 0.117 \text{ MeV}/\hbar$  and (b)  $\omega = 0.234 \text{ MeV}/\hbar$ .

$\gamma = -30^\circ$  support these configuration assignments.

### A. Triaxial band 1

A  $\nu i_{13/2} \otimes \pi(h_{11/2})^2$  structure has been previously associated with band 1 in  $^{133}\text{Ce}$  [7]. However, it is difficult to reconcile this configuration assignment with the contemporary data that exists in this mass region on rotational bands built upon the  $\nu i_{13/2}$  intruder orbital. In particular, rotational bands have been observed in  $^{131,132,133}\text{Ce}$  which are thought to be based on  $\nu i_{13/2}$ ,  $\nu(i_{13/2})^2$ , and  $\nu(i_{13/2})^2 \nu f_{7/2}$  configurations, respectively, with deformations measured to be  $\beta_2 \approx 0.4$  [18,11]. The different behavior of the  $\mathcal{J}^{(2)}$  moment of inertia of the  $^{133}\text{Ce} \Delta E_\gamma \sim 100 \text{ keV}$  band compared to the  $\nu i_{13/2}$  superdeformed bands in the Ce isotopes shown in Fig. 5 suggests a somewhat different high- $j$  configuration for this band.

To resolve the configuration assignment for band 1 in  $^{133}\text{Ce}$  total Routhian surface calculations for this nucleus were performed for the four lowest  $(\pi, \alpha)$  combinations. These calculations predict very  $\gamma$ -soft oblate/triaxial minima with  $\beta_2 \sim 0.19$ ,  $\gamma \sim -70^\circ$  to  $-90^\circ$  which are yrast or, near yrast, for all  $(\pi, \alpha)$  configurations in the rotational frequency

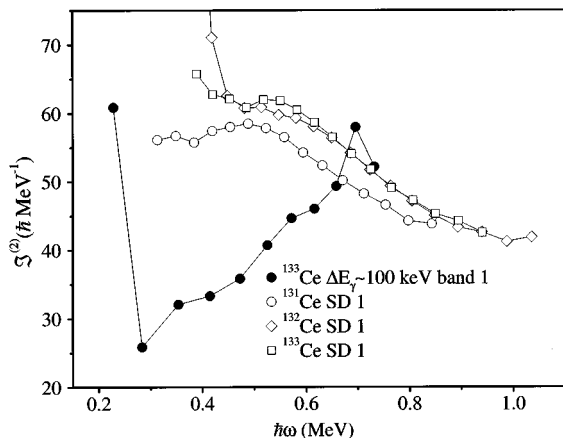


FIG. 5. A comparison between the dynamic moments of inertia of triaxial band 1 and the  $\nu(i_{13/2})^n$  bands in  $^{131,132,133}\text{Ce}$ .

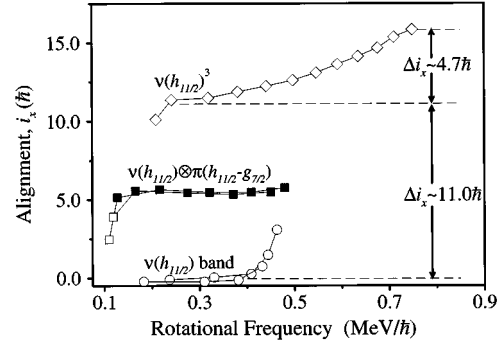


FIG. 6. Experimental alignment for triaxial band 1 and the  $\nu h_{11/2}$  band in  $^{133}\text{Ce}$  are plotted as a function of rotational frequency. The alignment of both signatures of the side band 1 in  $^{133}\text{Ce}$ , the reference band, are also shown. The filled points indicating the states over which the Harris parameters were fitted.

range  $0.23 \leq \hbar\omega \leq 0.45 \text{ MeV}$ ; see Fig. 4. This minimum is associated with a  $\nu(h_{11/2})^3$  configuration. The alignment of a pair of high- $\Omega$  quasineutrons would be expected to exert a strong  $\gamma$ -driving force upon the nuclear core inducing a shape change from  $\gamma \sim -30^\circ$  for the  $\nu h_{11/2}$  band to  $\gamma \sim -80^\circ$  for the three quasineutron band. Indeed, cranked Woods-Saxon calculations performed with pairing and the deformation parameters associated with the  $\nu h_{11/2}$  configuration ( $\beta_2 = 0.18$  and  $\gamma = -30^\circ$ ) predict a  $\nu(h_{11/2})^3$  alignment at  $\hbar\omega \sim 0.3 \text{ MeV}$ . To determine whether the  $\nu(h_{11/2})^3$  configuration corresponds to band 1 a comparison between the experimental and theoretical alignment gains  $\Delta i_x$  for the  $\nu(h_{11/2})^2$  crossing needs to be made. As stated above, this alignment has a strong  $\gamma$ -driving effect on the core and the complication of a suitable reference arises. However, since all the low-lying structures are based on a  $\gamma = -30^\circ$   $\nu h_{11/2}$  configuration the only choice available is to use a  $\gamma = -30^\circ$  reference. Therefore, when making a comparison between the theoretical and experimental  $\Delta i_x$  the different  $\gamma$ -deformations of the structures involved must be taken into account.

The experimental alignment for triaxial band 1 is presented in Fig. 6 as a function of rotational frequency. This plot was produced using Harris parameters of  $\mathcal{J}_0 = 21.9 \hbar^2 \text{ MeV}^{-1}$  and  $\mathcal{J}_1 = 11.1 \hbar^4 \text{ MeV}^{-3}$ , obtained by fitting levels above the  $19/2^+$  state in the  $\nu h_{11/2} \otimes \pi h_{11/2} \otimes \pi g_{7/2}$  side band, with  $\langle K \rangle = 5/2$ . It was also assumed that the lowest observed state in triaxial band 1 has  $I = 27/2 \hbar$ . From these data, the experimental alignment gain for triaxial band 1 relative to the  $\nu h_{11/2}$  band has been deduced to be approximately  $11 \hbar$ .

Cranked Woods-Saxon calculations performed with a reduced pairing,  $\Delta'_n(\omega) = 0.7 \times \Delta_n(\omega)$ , and the deformation parameters  $\beta_2 = 0.18$  and  $\gamma = -30^\circ$  predict a gain in alignment of  $\sim 4.5 \hbar$  for the  $\nu(h_{11/2})^2$  crossing, while  $\Delta i_x \sim 8.0 \hbar$  is predicted with  $\beta_2 = 0.18$  and  $\gamma = -80^\circ$ . In addition, the shape change will also affect the contribution to the aligned angular momentum of the 75th neutron, occupying the  $[514]9/2^- \alpha = -1/2$  orbital. Therefore, the total alignment gain expected for the  $\nu(h_{11/2})^2$  crossing, in conjunction with the associated shape change, is  $\Delta i_x \sim 7.5 - 11.0 \hbar$ . From the reasonable agreement between theory and experiment a

structural assignment of  $\nu(h_{11/2})^3$  is proposed for triaxial band 1. The gradual alignment of  $s_{1/2}$  and  $d_{3/2}$  neutron pairs are thought to be partially responsible for the smooth increase in the alignment of triaxial band 1; see Fig. 6.

A mean transitional quadrupole moment  $Q_t \approx 2.3 e b$  has been measured for band 1 [12]. For nonaxial symmetric shapes the intrinsic quadrupole moment  $Q_o$  is related to the transitional quadrupole moment  $Q_t$  by

$$Q_o = \frac{\sqrt{3}Q_t}{2\cos(\gamma + 30^\circ)} \quad (1)$$

and the value of the intrinsic quadrupole moment is related to the ellipsoidal deformation parameter  $\beta_2$  by

$$Q_o = \frac{3}{\sqrt{5}\pi} ZR_o^2 \beta_2 \left( 1 + \frac{1}{8} \sqrt{\frac{5}{\pi}} \beta_2 + \frac{5}{8\pi} \beta_2^2 + \dots \right). \quad (2)$$

From these relationships the quadrupole deformation for triaxial band 1 has been extracted to be  $\beta_2 = 0.18$ , using  $\gamma = -80^\circ$ , in good agreement with the predictions of the total Routhian surface calculations for the  $(\pi, \alpha) = (-, -1/2)$  three quasineutron structure further corroborating the  $\nu(h_{11/2})^3$  configuration assignment to this band.

### B. Triaxial bands 2 and 4

Both bands are observed to primarily depopulate into triaxial band 1 (see Fig. 3) and consequently their structures are believed to be closely related to that of this band. It has not been possible to determine the ordering of the 882 doublet and the 892.4 keV transitions in band 2. Therefore the assumption has been made that there is a monotonic increase in transition energy with increasing spin. Furthermore, these transitions are also believed to be E2's from the similarity of their intensities and the detector geometry. (The majority of the detectors in the early implementation phase of GAMMASPHERE were positioned at forward and backward angles favouring the detection of E2's over M1's.) Band 2 is therefore suggested to have  $(\pi, \alpha) = (-, -1/2)$ . The similarity of the behavior of bands 2 and 4 leads to the speculation that these bands are signature partners. This implies that the unseen transitions in each of the decay paths between bands 4 and 1, indicated in Fig. 3, total an odd value of spin. The experimental alignments of bands 2 and 4 relative to triaxial band 1, obtained using the Harris parameters given in Sec. IV A and  $\langle K \rangle = 5/2$ , are shown in Fig. 7. The alignment gains for triaxial bands 2 and 4 relative to band 1 have been extracted to be  $\Delta i_x \sim 4.0\hbar$  and  $\sim 3.2\hbar$ , respectively. It was assumed the unseen linking transitions in each decay path from band 4 to band 1 contribute  $3\hbar$ . A spin of  $41/2\hbar$  is therefore assigned to the lowest observed level in band 4. (An alignment gain of  $\sim 1.2\hbar$  would be extracted for band 4 if the linking transitions contribute only  $1\hbar$ . This would be in conflict with the earlier speculation that bands 2 and 4 are signature partners.)

In order to try and identify the nature of the particles aligning at  $\hbar\omega \sim 0.45$  MeV, cranked Woods-Saxon calculations have also been performed with pairing at  $\beta_2 = 0.18$  and  $\gamma = -80^\circ$  for protons. These calculations predict the align-

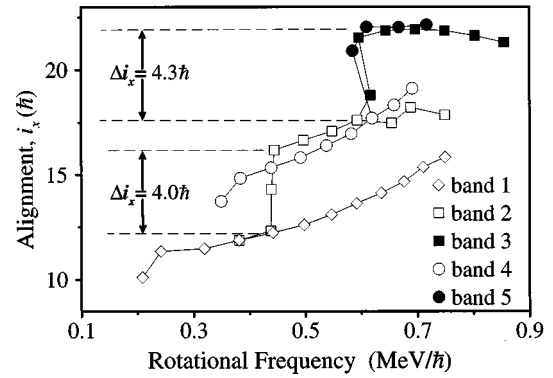


FIG. 7. Experimental alignment for triaxial bands 1–5 in  $^{133}\text{Ce}$  are plotted as a function of rotational frequency. The Harris parameters used to obtain this plot were  $\mathcal{J}_0 = 21.9\hbar^2 \text{ MeV}^{-1}$  and  $\mathcal{J}_1 = 11.1\hbar^4 \text{ MeV}^{-3}$ .

ment of pairs of  $d_{5/2}$ ,  $g_{7/2}$ , and  $h_{11/2}$  protons at  $\hbar\omega \approx 0.6$ ,  $\hbar\omega \approx 0.65$ , and  $\hbar\omega \approx 0.6$ , respectively. Unlike the  $d_{5/2}$  and  $h_{11/2}$  quasi-proton alignments, the  $g_{7/2}$  alignment has almost no shape driving effect on the nuclear core at  $\gamma \sim -80^\circ$ . However, the proton  $d_{5/2}$  alignment tends to drive the core shape from  $\gamma \sim -80^\circ$  to  $\gamma \sim -120^\circ$ , and the alignment of a pair of low- $\Omega$   $h_{11/2}$  protons has the opposite  $\gamma$ -driving effect, preferring  $\gamma \sim -30^\circ$ . Cranked Woods-Saxon calculations performed at  $\beta_2 = 0.18$  and  $\gamma = -120^\circ$ , with pairing, predict the  $d_{5/2}$  crossing to occur at  $\sim 0.55$  MeV, while similar calculations performed at  $\gamma = -30^\circ$  predict the  $\pi h_{11/2}$  alignment to occur at the lower rotational frequency of  $\hbar\omega \approx 0.4$  MeV. It is therefore the  $\pi(h_{11/2})^2$  alignment that is currently thought to result in the population of triaxial bands 2 and 4 from triaxial band 1. The rotational alignment of a pair of  $h_{11/2}$  protons is predicted to contribute  $\sim 6-8.8\hbar$  to the aligned angular momentum, depending on the degree of  $\gamma$  deformation. However, the change in  $\gamma$  deformation ( $\gamma = -80^\circ \rightarrow -30^\circ$ ) associated with the  $\pi(h_{11/2})^2$  crossing causes the contribution to the aligned spin of the  $\nu(h_{11/2})^3$  quasiparticles to be reduced by  $\sim 5.0\hbar$ . This results in an effective alignment gain of  $\Delta i_x \sim 1.0-3.8\hbar$  for the  $\pi h_{11/2}$  protons, in reasonable agreement with the experiment values. The 5 quasiparticle structure  $\nu(h_{11/2})^3 \otimes \pi(h_{11/2})^2$  has therefore been tentatively assigned to triaxial bands 2 and 4.

### C. Triaxial bands 3 and 5

A feature common to both triaxial bands 2 and 4 is a band crossing at  $\hbar\omega \sim 0.6$  MeV resulting in the population of triaxial bands 3 and 5, respectively (see Fig. 3). This backband is more easily seen in Fig. 7, and is thought to arise from the alignment of a pair of  $g_{7/2}$  protons. The  $g_{7/2}$  proton alignment has little  $\gamma$ -driving effect on the core at the  $\gamma$ -deformation at which bands 2 and 4 are thought to reside, namely  $\gamma \sim -30^\circ$ . The alignment gain at  $\gamma \sim -30^\circ$  associated with the  $g_{7/2}$  crossing is predicted to be  $\sim 5.0\hbar$ , in good agreement with the experimental value of  $\Delta i_x \sim 4.3\hbar$ . The triaxial bands 3 and 5 are therefore tentatively assigned the 7 quasiparticle  $\nu(h_{11/2})^3 \otimes \pi(h_{11/2})^2 \otimes \pi(g_{7/2})^2$  structure.

### D. Triaxial band 6

The principal decay path of this band feeds into the  $\nu h_{11/2} \otimes \pi(h_{11/2})^2$  side band and therefore triaxial band 6 is

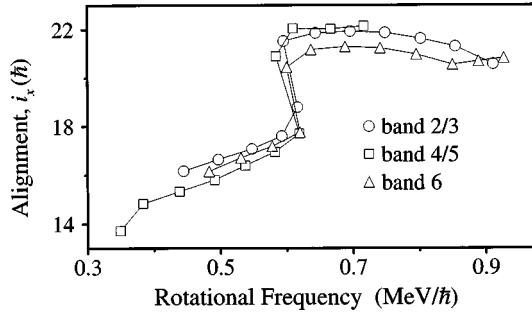


FIG. 8. Experimental alignment for triaxial bands 3, 5, and 6 in  $^{133}\text{Ce}$  plotted as a function of rotational frequency. The Harris parameters used to obtain this plot were  $\mathcal{J}_0 = 21.9\hbar^2 \text{ MeV}^{-1}$  and  $\mathcal{J}_1 = 11.1\hbar^4 \text{ MeV}^{-3}$ . For bands 3 and 5  $\langle K \rangle = \frac{5}{2}$  was used, while  $\langle K \rangle = \frac{1}{2}$  and an initial spin of  $\frac{49}{2}$  was used for band 6.

expected to have a configuration based on this structure. The absence of any signature splitting observed for the  $\nu h_{11/2} \otimes \pi(h_{11/2})^2$  side bands suggests that this configuration has a near prolate shape ( $\gamma \sim 0^\circ$ ), since the signature splitting due to the odd neutron is expected to fall to zero at this  $\gamma$  deformation. Paired Woods-Saxon calculations performed with  $\beta_2 = 0.18$ ,  $\gamma = 0^\circ$  indicate that band 6 could be built on the  $\nu(h_{11/2})^2 \otimes \nu s_{1/2} \otimes \pi h_{11/2}^2$  structure. Again, the occupation of an additional  $h_{11/2}$  neutron orbital is expected to drive the nucleus from  $\gamma \sim 0^\circ$  towards  $\gamma \sim -30^\circ$ , resulting in a minimum at deformation parameters similar to those at which bands 3 and 5 are believed to reside. In view of the behavior exhibited by bands 3 and 5, a backbend could be expected, and is indeed observed, to occur in band 6 at  $\hbar\omega \sim 0.6 \text{ MeV}$ . The similarity of the alignment of band 6 and triaxial bands 3 and 5, see Fig. 8, suggests the backbend observed in band 6 is also due to the alignment of a pair of  $g_{7/2}$  protons. A configuration of  $\nu(h_{11/2})^2 \otimes \nu s_{1/2} \otimes \pi(h_{11/2})^2 \otimes \pi(g_{7/2})^2$  is therefore proposed for band 6 after the observed backbend.

### E. Triaxial band 7

Band 7 is observed to primarily depopulate into the positive parity low-lying  $\nu h_{11/2} \otimes \pi h_{11/2} \otimes \pi g_{7/2}$  side band and is therefore thought to be related to this structure. The occupation of the favoured  $h_{11/2}$  and  $g_{7/2}$  quasiproton orbitals blocks both of the  $h_{11/2}$  and  $g_{7/2}$  proton alignments discussed above. Again, this configuration is thought to be prolate because of the lack of signature splitting of  $\nu h_{11/2} \otimes \pi h_{11/2} \otimes \pi g_{7/2}$  side bands. Therefore, cranked Woods-Saxon calculations with pairing have been performed for both protons and neutrons at  $\beta_2 = 0.18$  and  $\gamma = 0^\circ$  in order to determine the structure of band 7. These calculations suggest that triaxial band 7 could be based on the  $\nu(h_{11/2})^2 \otimes \pi h_{11/2} \otimes \nu s_{1/2} \otimes \pi g_{7/2}$  5 quasiparticle configuration.

## V. SUMMARY

In summary, seven rotational structures with energy spacings of  $\Delta E_\gamma \sim 100 \text{ keV}$  have been observed in  $^{133}\text{Ce}$ . The most intensely populated of these bands, band 1, has been tentatively assigned a  $\nu(h_{11/2})^3$  configuration. Bands 2 and 4,

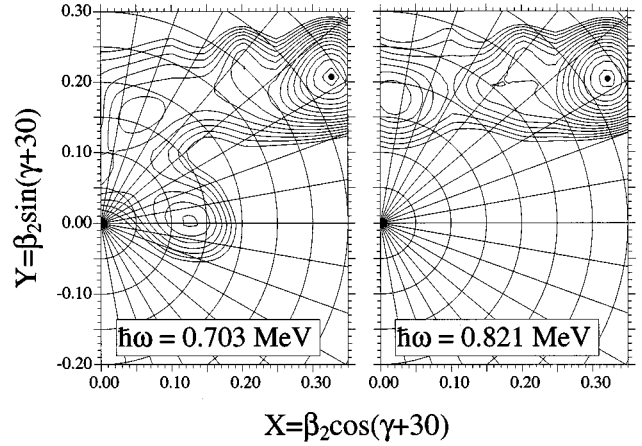


FIG. 9.  $^{133}\text{Ce}$  total Routhian surface calculations with the odd neutron occupying the lowest  $(\pi, \alpha) = (-, -\frac{1}{2})$  orbital.

which feed into band 1, are suggested to be built on either signature of the related  $\nu(h_{11/2})^3 \otimes \pi(h_{11/2})^2$  configuration. A  $\pi(g_{7/2})^2$  alignment is currently thought to be responsible for the backbend observed in bands 2 and 4 at  $\hbar\omega \sim 0.6 \text{ MeV}$  resulting in the population of triaxial bands 3 and 5, respectively. The backbend observed in band 6 at  $\hbar\omega \sim 0.6 \text{ MeV}$  is also believed to be due to the alignment of a pair of  $g_{7/2}$  protons. A configuration of  $\nu(h_{11/2})^2 \otimes \nu s_{1/2} \otimes \pi(h_{11/2})^2 \otimes \pi(g_{7/2})^2$  is therefore proposed for band 6 after the observed backbend, while band 7 is tentatively assigned a  $\nu(h_{11/2})^2 \otimes \nu s_{1/2} \otimes \pi h_{11/2} \otimes \pi g_{7/2}$  structure. However, the exact nature of these bands is still an open question. The observation of similar structures in neighbouring nuclei will be crucial in order to aid firm configuration assignments to all the bands.

Finally, it is interesting to note that at high rotational frequency the total Routhian surface calculations predict that there are weak noncollective oblate minima ( $\gamma \sim +60^\circ$ ) for all  $(\pi, \alpha)$  combinations; see Fig. 9. This leads to the speculation that these minima are associated with the complete alignment of the spin vectors of the particles making up the various triaxial configurations. An experiment on a large array may enable the terminating states for some of these structures to be observed. This would provide the first opportunity to study such ‘‘soft band’’ termination outside the  $A \sim 110$  region [19]. Recent calculations by Afanasjev and Ragnarsson [20] also indicate that a new region of ‘‘soft’’ termination should exist around  $Z = 57-61$  and  $N = 72-79$ .

## ACKNOWLEDGMENTS

This work was supported in part by the U.S. National Science Foundation and by the U.K. Engineering and Physical Science Research Council, from which A.T.S. and L.W. acknowledge financial support. The receipt of financial support from the University of York is acknowledged by K.H. We also wish to thank Dr. Ramon Wyss for helpful discussions, the Lawrence Berkeley 88 in. cyclotron accelerator crew for providing beam and support, and R. Darlington for the production of the target.

- [1] I. Ragnarsson, A. Sobiczewski, R.K. Sheline, S.E. Larsson, and B. Nerlo-Pomorska, Nucl. Phys. **A233**, 329 (1974).
- [2] Y.S. Chen, S. Frauendorf, and G.A. Leander, Phys. Rev. C **28**, 2437 (1983).
- [3] D.B. Kern, R.L. Mlekodaj, G.A. Leander, M.O. Kortelahti, E.F. Zganjar, R.A. Braga, R.W. Fink, C.P. Perez, W. Nazarewicz, and P.B. Semmes, Phys. Rev. C **36**, 1514 (1987).
- [4] R. Wyss, J. Nyberg, A. Johnson, R. Bengtsson, and W. Nazarewicz, Phys. Lett. B **215**, 211 (1988).
- [5] G.A. Leander, S. Frauendorf, and F.R. May, in *Proceedings of the Conference on High Angular Momentum Properties of Nuclei (Oak Ridge), 1982*, edited by N.R. Johnson (Harwood Academic, New York, 1983), p. 281; S. Frauendorf and F.R. May, Phys. Lett. **125B**, 245 (1983).
- [6] S. Åberg, Phys. Ser. **25**, 23 (1982).
- [7] R. Ma, E.S. Paul, C.W. Beausang, S. Shi, N. Xu, and D.B. Fossan, Phys. Rev. C **36**, 2322 (1987).
- [8] R. Ma, E.S. Paul, D.B. Fossan, Y. Liang, N. Xu, R. Wadsworth, I. Jenkins, and P.J. Nolan, Phys. Rev. C **41**, 2624 (1990).
- [9] P.J. Nolan, A.J. Kirwan, D.J.G. Love, A.H. Nelson, D.J. Unwin, and P.J. Twin, J. Phys. G **11** L17 (1985).
- [10] Y-X. Luo, J-Q. Zhong, D.J.G. Love, A.J. Kirwan, M.J. Godfrey, I. Jenkins, P.J. Nolan, S.M. Mullins, and R. Wadsworth, Z. Phys. A **329**, 125 (1988).
- [11] K. Hauschild *et al.*, Phys. Lett. B **353**, 438 (1995).
- [12] J. Nyberg *et al.*, The Niels Bohr and NORDITA Research Activity report, 1990 (unpublished), p. 63.
- [13] K. Hauschild *et al.*, Phys. Rev. C **52**, R2281 (1995).
- [14] M.A. Delaplanque and R.M. Diamond, Lawrence Berkeley Laboratory, Berkeley, Report No. PUB-5202, 1988 (unpublished).
- [15] D.C. Radford, Nucl. Instrum. Methods A **361**, 297 (1995).
- [16] J.N. Wilson, Ph.D. thesis, University of Liverpool, 1995.
- [17] J. Nyberg *et al.*, The Niels Bohr and NORDITA Research Activity report, 1989 (unpublished), p. 85.
- [18] R.M. Clark *et al.*, Phys. Rev. Lett. **76**, 3510 (1996).
- [19] I. Ragnarsson, V.P. Janzen, D.B. Fossan, N.C. Schmeing, and R. Wadsworth, Phys. Rev. Lett. **74**, 3935 (1995).
- [20] A.V. Afanasjev and I. Ragnarsson, Nucl. Phys. **A529**, 315 (1995).